

Damage tolerance analysis of a cracked attachment lug using BEM

A. Apicella, S. Magliaro

ALENIA Azienda Finmeccanica, Pomigliano d'Arco, Naples, Italy

ABSTRACT

A detailed 3D analysis using BEM (Boundary Element Method) was performed to determine the stress distribution and SIFs of a corner crack of the fuselage to wing attachment lug of a medium range military transport aircraft. The contact pin-lug has been studied with non-linear contact analysis. Based on this study a crack growth prediction has been performed with a proper analytical model. For the above prediction, both constant and variable amplitude loads were considered. An experimental correlation has been made for both crack growth and final fracture of the component.

As a result of the present work it can be concluded the industrial feasibility of fracture mechanics analyses using BEM.

In fact a good agreement has been reached with the available experimental results. Also it can be concluded that the interference-fit pin installation causes a significative decrease in the stress intensity factor range and hence improvements in the fatigue crack growth life. The elasto-plastic CORPUS model will be used to predict crack growth evolution.

Nomenclature :

a	crack depth length	μ	shear modulus
C	surface crack length	ν	Poisson's ratio
DLL	design limit load	Q2	Beasy linear order element
DK	S. I.F. range	Q38	Beasy reduced quadratic order element
E	Young's modulus	SIF	stress intensity factor
KI	mode I stress intensity factor		

DISCUSSION

Structural fatigue often initiates in areas of high stress concentration caused by the bearing load of pins. The above causes a small crack initiation time and crack growth life.

The main purpose of this report is to validate the Fracture Mechanics tool proposed by ALENIA. The method uses BEM for SIF evaluation and an elasto-plastic crack propagation

model for the life prediction under spectra and constant amplitude loads.

A three-dimensional BEM analysis using BEASY code, an engineering analysis system based on the Boundary Element Method has been performed in order to determine the stress distribution in the selected component in presence of a crack and under contact conditions. Even if a number of studies and analytical results are available in literature, the capability of a full BEM analysis gives more understanding results.

Hereafter the contents, method and the results of the analysis are described. The component selected for the analysis is the fuselage to wing attachment of a medium range military transport aircraft for which results are known from an experimental test program.

LUG COMPONENT DESCRIPTION

Fig.1 shows the detailed geometry of the component. The lug is made of 7075-T73511 forged aluminum alloy for which Young modulus is 71 GN/m^2 and Poisson ratio is 0.3, with a hole diameter of 25.5 mm. The pin and the bushing are both of 15-5-PH steel with Young modulus equal to 210 GN/m^2 and Poisson ratio to .33.

The lug component has been tested with an initial corner flaw of $1.27 \times 1.27 \text{ mm}$ under a variable amplitude spectrum coming from in service monitoring. The same test article was also tested with constant amplitude load cycles. The test apparatus used consists, mainly, of a rigid beam fixed on the ground on which both the test article and the hydraulic jack have been installed. The upper end of the test article has been constrained through fasteners to a strong back while the lug lower end has been joined to the stroke of the hydraulic jack.

BOUNDARY ELEMENT MODELS

BEM is an integral differential equation method based on the formulation reported below :

$$C_k u_k + \sum_{j=1}^N \int_{\Gamma_j} T^* u \, dS = \sum_{j=1}^N \int_{\Gamma_j} U^* t \, dS.$$

in which Γ_j are segments in which boundary S is subdivided and C_k is a constant linked to the source point, while u and t are displacements and tractions vectors.

BEASY is an engineering analysis system based on this method. ,,

The surface description of the model was realized directly in BEASY-IMS, the interactive modeling environment of BEASY software, and post-processing ensures an easy way to visualize results, in particular stress intensity factors.

The model was divided into three distinct zones or substructures: the main body of the lug, the lug upper side and the pin. This feature makes easier crack tip modeling as well as full model handling (see fig. 2).

Different models have been realized with various crack sizes. In

order to have the best sensitivity to the fracture mechanics parameters and the best correlation with the experimental results, different order of elements and boundary conditions at lug-pin interface have been used. In fact near crack front reduced quadratic elements are preferable instead of linear ones. The model has been restrained in all 3 directions in the holes. In order to have a simpler model, only the last three rows of holes have been modeled. The latter together with the pin loading creates a secondary bending in the structure causing an higher stress on a surface than on the opposite one.

The load has been introduced in the model as a pin body load equal to a reference load of 5908 daN. This value correspond to the 38% of the design limit load.

MACRO-ELEMENT FOR AUTOMATIC CRACK TIP MODELING

In order to have a quick crack tip modeling it has been created a short fortran code which creates the crack geometry and the mesh automatically. The code generates a crack tip mesh of a whatever semi-elliptical aspect to be inserted wherever in the full model through simple modifications. A proper mesh grading ranging from 1/10 to 1/20 of the crack depth length can be generated near the crack front using different element types. In fig. 3 are shown the various crack fronts used in the analysis.

INTERFERENCE-FIT LUG-PIN EFFECTS

The component previously described is characterized from the installation of an interference-fit bushing in which the loaded pin acts. Such installation can reduce the effective tangential stress at the likely location of crack initiation causing improvements in fatigue and crack growth life and reducing fretting damage on the hole wall of the lug.

Very few solutions are available for estimating stress intensity factors for cracks at attachment lugs having interference effects. In fact the correct evaluation of the above requires elas-plastic tools in order to account the right stress distribution near the hole. But if the material is still in elastic regime, an adequate sensitivity on the stress distribution decrease could be reached even with linear elastic tools.

In fact SIFs for the structure can be evaluated using Buckner's weight function given by the following relation

$$m(x,a) = \frac{H \partial u(x,a)}{2K \partial a}$$

where H equals E for plane stress and $E/(1-\nu^2)$ for plane strain, $u(x,a)$ is the crack opening displacement at x for a crack length a. The integral of the product of this function and the stress distribution along the crack boundary gives the stress intensity factor which in equation form is :

$$K = \int_a p(x) m(x,a) dx$$

where $p(x)$ is the stress distribution that would exist along the crack boundary if the crack were not there.

RESULTS OF BEM ANALYSIS

Summary of timings for the different analysis performed are shown in the diagram shown in figure 4.

The above has run on an IBM RISC560 computer which is a medium range workstation with a performance figure of 30 Mflops. Fig.5 shows details of the elliptical crack model and the mesh used with a crack 1.27x1.27mm. The Von Mises stress distribution near the crack is shown in fig.6. The deformed geometry of the complete model with a crack depth length of 21 mm and an aspect ratio $a/c=1.288$ is shown in fig.7.

SIFs are evaluated through Irwin's equations. For example in the twodimensional case, once the displacements normal to the crack line have been evaluated, SIF for mode I is given from :

$$v = \frac{K_I}{4\mu} \sqrt{\frac{r}{2\pi}} \left\{ (2\kappa - 1) \sin \frac{\theta}{2} - \sin \frac{3\theta}{2} \right\} + \dots$$

Summary of SIFs results with both displacement and stress based methods along the crack front are shown in the diagram of fig.8 for the initial crack size. Table 1 shows results for the different crack sizes.

All results are obtained by using a non-linear contact condition at pin-lug interface. The non-linear solution provides the exact contact area between the pin and the main body of the model. From the results it can be concluded that best results are those with non-linear contact analysis and reduced quadratic elements.

Further more stable results for SIFs are those obtained through the displacements based method.

CRACK GROWTH PREDICTION AND TEST CORRELATION

Aircraft load spectrum. The lug was tested for a military transport aircraft spectrum.

The in flight load spectrum represents in terms of frequencies the gust and maneuvers spectra combined with loads due to the differential pressure in each flight. The above comes from in service monitoring. Negative loads due to ground loads conditions have been omitted both in the experimental test and analytical prediction. In fig.9 the cumulative peak exceedances per 785 flights are given in terms of percent of design limit load (DLL). The DLL for the lug was 15270 daN which corresponds to 77.9 MPa.

Next paragraph describes an analytical elastoplastic crack growth model which can perform predictions accounting for retardation effects.

CORPUS model description. As consequence of the crack closure model, the crack extension in every cycle is determined by the effective stress range.

In cycle (i) is :

$$Da / Dn = C_i Dk_{eff}^n$$

The cycle (i) is defined by a maximum $S_{max,i}$ followed by a minimum $S_{min,i}$. The effective stress range is determined as

$$\begin{aligned}
 DS_{\text{eff},i} &= S_{\text{max},i} - S_{\text{min},i-1} & \text{if } S_{\text{op}} < S_{\text{min},i-1} \\
 DS_{\text{eff},i} &= S_{\text{max},i} - S_{\text{op}} & \text{if } S_{\text{min},i-1} < S_{\text{op}} < S_{\text{max},i} \\
 DS_{\text{eff},i} &= 0 & \text{if } S_{\text{op}} \geq S_{\text{max},i}
 \end{aligned}$$

where SOP is the maximum crack opening stress level, which will be described below.

The corpus model is basically associated with plastic deformation left in the wake of the crack (Elbert mechanism). It is assumed that each cycle will leave its own plastic deformation, including its reversed plastic deformation during unloading.

When the crack is growing, plastic deformation of previous cycles will be left in the wake of the crack. According to the Corpus model the wake of the crack is covered with humps where each hump is associated with a previous cycle. The humps is created during uploading, while reversed flow during unloading will reduce the hump. Figure 10 shows three humps in the wake of the crack. A crack is considered to be just opened during uploading when the last hump loses contact. It implies that :

$$S_{\text{op}} = S_{\text{op}}^3 \text{ or } SOP = \max S_{\text{op}}^n$$

In CORPUS model a peak load will activate a delay switch which is turned off if the crack has grown through the plastic zone of the peak load.

$$\begin{aligned}
 S_{\text{op}}^n &= g(S_{\text{max}}^n, S_{\text{min}}^n) * h & \text{if } a^n \leq a \leq a^n + D^n \\
 S_{\text{op}}^n &= 0 & \text{if } a > a^n + D^n
 \end{aligned}$$

where D^n is the retardation region (plastic zone) and $g(S_{\text{max}}^n, S_{\text{min}}^n)$ is the hump opening function. Based on empirical evidence the function was defined as :

$$\begin{aligned}
 g(S_{\text{max}}^n, S_{\text{min}}^n) &= S_{\text{max}}^n (-0.4 R^4 + 0.9 R^3 - 0.15 R^2 + 0.2 R + 0.45) & \text{if } R > 0 \\
 g(S_{\text{max}}^n, S_{\text{min}}^n) &= S_{\text{max}}^n (0.15 R^2 + 0.2 R + 0.45) & \text{if } -0.5 \leq R \leq 0 \\
 \text{and } h &= 1 - 0.2(1 - R^n)^3 * (S_{\text{max}}^n / 1.15 F_{ty})^3
 \end{aligned}$$

where R is the stress ratio ($S_{\text{min}}^n / S_{\text{max}}^n$). The same function was supposed to be applicable to both 2024-T3 and 7075-T6.

Crack growth predictions.

The DK value for each cycle in the flight-by-flight spectrum was determined using the stress intensity computation procedures detailed in the previous section. These were then used to obtain the crack growth extension for each cycle. Displacement based SIFs were used in the crack growth integration which agrees with the experimental result of 9500 flights until a growing crack of 2x3mm was measured with rotor test. Further in fig. 11 is shown crack growth with SIFs accounting for the interference fit-bushing effect described in previous section.

After crack inspection and new interference-fit pin installation a static test was performed which resulted in a large plastic zone ahead crack tip. Again load spectrum was applied and

crack growth retardation, due to the periodically applied higher load levels was taken into account using the elasto-plastic model described. The calculation has shown that remarkable retardation effects occur for the load spectrum considered with a 3x2 mm flaw size so that no growth resulted.

Further load cycles of constant amplitude were applied at $R=0.05$ with a maximum load equal to 59% of DLL, i.e. 9000 daN.

The above resulted in around 36200 experimental crack growth cycles. Both experimental and analytical results from BEM are shown in fig.12, from which crack growth obtained using displacement based SIFs is closer to the test results. Probably a more accurate catching of stress based SIFs could give better results. In fact the latter ones are almost unstable near the crack front so that not always an accurate SIF value based on this method could be extracted. Nevertheless it must be remarked that both methods give conservative crack growth predictions.

As regard component final fracture it can be seen that the value of SIF at the final corner flaw size of 21x16.3 mm is equal to $499.5 \text{ N/mm}^{3/2}$ at 26% of DLL. The toughness allowable obtained from CCT specimens was $2120 \text{ N/mm}^{3/2}$, so that from BEM results a critical load of 25050 daN has been obtained, while the experimental critical load was 25200 daN corresponding to 1.65% of DLL.

CONCLUSIONS

The BEM method and CORPUS model were used to correlate the experimental results of a wing attachment lug. The accuracy obtained was about +5 percent or better. The results were qualitatively consistent with other studies.

A quantitative comparison is difficult because the geometry was not the same. The time spent in work is acceptable and the accuracy high.

References

- [1] Smith R. N. L., Aliabadi M. H., "Boundary Integral equation methods for the solution of crack problems", *Mathl. Compu t. Modeling*, vol. 15, No 3-5, pp.285-293, 1991
- [2] BEASY, Boundary Element Analysis System Software. Computational Mechanics, Southampton U.K.
- [3] Hsu, T.M. & Kathiresan K., "Analysis of cracks at an attachment Lug having an interference-fit bushing", ASTM STP 791 1983, pp. I 172-193
- [4] Bueckner, H. F., "Weight Functions for the Notched bar", 1971
- [5] Tada H., Paris P.C., and Irwin G. R., *The Stress Analysis of Cracks Handbook*, Del Research Corp., 1973
- [6] Univ. di Napoli "Federico II", Facoltà di Ingegneria Ist. di Costruzioni di Macchine, Thesis: "Sulla propagazione delle cricche di fatica correlata ai modelli di crack closure", 1992-1993
- [7] Dipartimento di Ing. Aerospaziale, Univ. di Pisa, "Risultati delle prove di propagazione della fessura in elementi di forte spessore di cui all'AEPE N.52-06-20-06", Sett. 1983

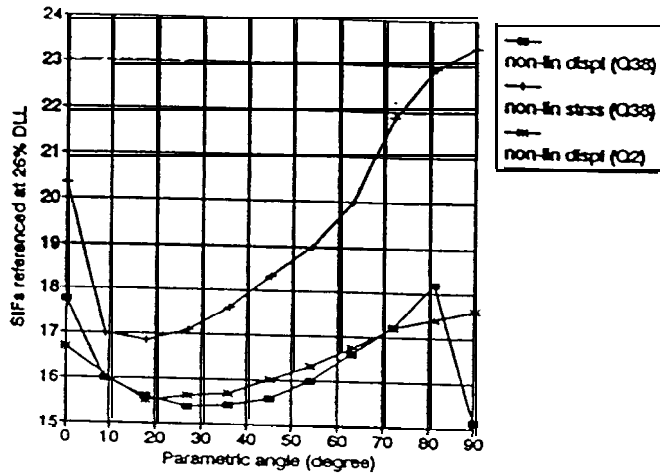
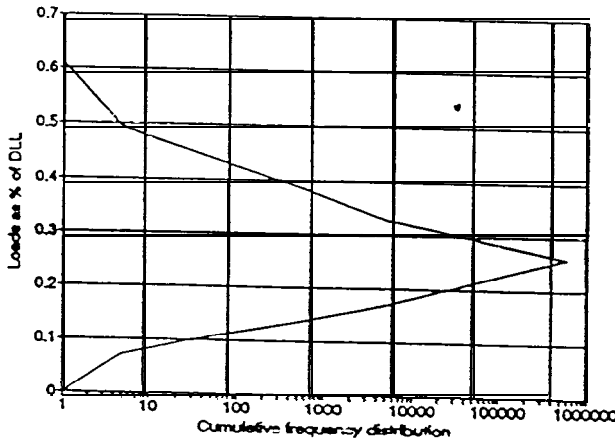


Fig. 8 - Lug model displaced shape with the critical flaw size.

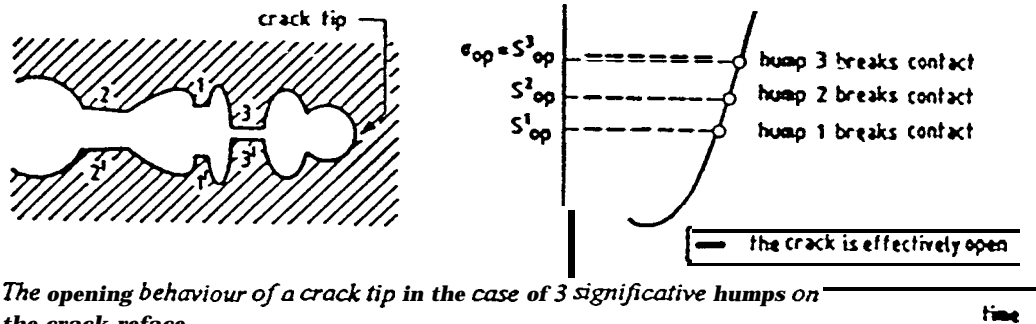
Fig. 7 - Displacements and stress based SIFs around 1.27x1.27 crack front.



a x c crack (mm)	KI at surface C (N/mm ^{3/2})
1.27 x 1.27	177.4
2 x 1.6	184.3
3 x 2	203.4
7.16 x 5.04	242
15.36 x 11.3	287.3
21 x 16.3	499.5

Tab. 1

Fig. 9 - Cumulative peak exceedances per 785 flights.



The opening behaviour of a crack tip in the case of 3 significant humps on the crack reface

Fig.10 - Schematic of the Corpus Model

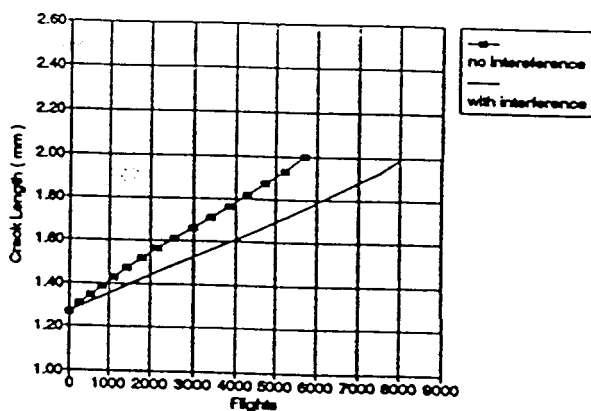


Fig.11 - Crack growth predictions

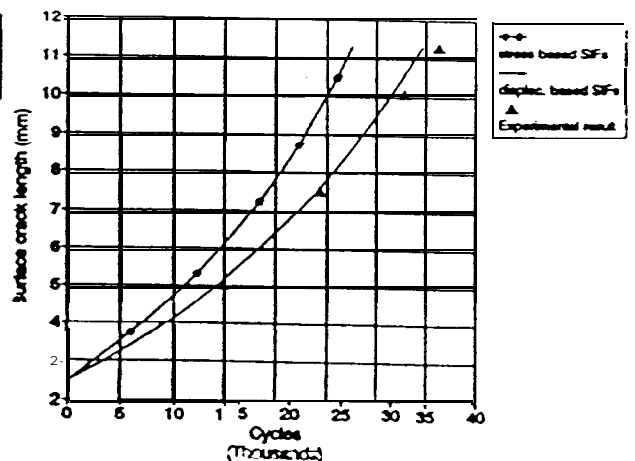


Fig.12 - Crack growth prediction under constant amplitude loads